Suppression of chaotic dynamics and localization of two-dimensional electrons by a weak magnetic field

M. M. Fogler, A. Yu. Dobin,* V. I. Perel,* and B. I. Shklovskii
Theoretical Physics Institute, University of Minnesota, 116 Church St. Southeast, Minneapolis, Minnesota 55455
(Received 19 February 1997)

We study a two-dimensional motion of a charged particle in a weak random potential and a perpendicular magnetic field. The correlation length of the potential is assumed to be much larger than the de Broglie wavelength. Under such conditions, the motion on not too large length scales is described by classical equations of motion. We show that the phase-space averaged diffusion coefficient is given by the Drude-Lorentz formula only at magnetic fields B smaller than certain value B_c. At larger fields, the chaotic motion is suppressed and the diffusion coefficient becomes exponentially small. In addition, we calculate the quantum-mechanical localization length as a function of B at the minima of σ_{xx}. At $B<B_c$ it is exponentially large but decreases with increasing B. At $B>B_c$, this decrease becomes very rapid and the localization length ceases to be exponentially large at a field B_*, which is only slightly larger than B_c. Implications for the crossover from the Shubnikov–de Haas oscillations to the quantum Hall effect are discussed. [S0163-1829(97)00735-2]

I. INTRODUCTION

In this paper we study a two-dimensional motion of a charged particle in a weak random potential and a perpendicular magnetic field. This problem has deep historical roots and the limiting cases of a weak and a very strong magnetic field are fairly well understood. As we will see below, the nature of the motion in these two limits is crucially different. Surprisingly, until now no theory for the crossover between the two limits has been proposed. Our goal is to develop such a theory. We will start with a classical description of the transport.

An important prediction of the classical magnetotransport theory is that the conductivity in the direction perpendicular to the magnetic field is reduced,

$$\sigma_{xx}=\frac{\sigma_0}{1+(\omega_c\tau)^2}, \tag{1.1}$$

where σ_0 is the zero-field conductivity (the magnetic field B is assumed to be along the $\hat{\boldsymbol{z}}$ direction), $\omega_c=eB/mc$ is the cyclotron frequency, and τ is the transport time determined by the properties of the random potential. Strictly speaking, in classical theory it is more consistent to study the diffusion coefficient D. So, we would write the Drude-Lorentz formula (1.1) in the form

$$D=\frac{D_0}{1+(\omega_c\tau)^2}, \tag{1.2}$$

where $D_0=\frac{1}{2}v^2\tau$ is the diffusion coefficient in zero field, v being the particle velocity. Drude-Lorentz formula predicts that if the magnetic field is not too weak so that $\omega_c\tau>1$, then the diffusion coefficient falls off inversely proportional to the square of the magnetic field.

Let us examine the physical picture of the motion in such magnetic fields. It is easy to verify that the Lorentz force has a dominant effect on the motion and the deviations from the perfectly circular cyclotron orbit are small. In such circumstances, the original coordinates $\boldsymbol{r}=(x,y)$ are not very useful anymore. Instead, it is convenient to study the motion of the guiding center $\boldsymbol{\rho}=(\rho_x,\rho_y)$ of the cyclotron orbit.

Suppose the cyclotron gyration is clockwise (this is the case if, e.g., the particle charge is negative and the magnetic field is in the negative $\hat{\boldsymbol{z}}$ direction). The guiding center coordinates are defined as follows:

$$\rho_x=x+\frac{v_y}{\omega_c}, \quad \rho_y=y-\frac{v_x}{\omega_c}. \tag{1.3}$$

Drude-Lorentz formula (1.2) results from the assumption that the guiding center $\boldsymbol{\rho}$ performs a random walk. The characteristic step of such a random walk is the cyclotron radius, $R_c=v/\omega_c$, and the time interval between the steps is the transport time τ. As we will see below, this is the correct description of the motion if the magnetic field is not too strong.

Perhaps the first work that demonstrated that the Drude-Lorentz formula may not be valid in the limit of strong magnetic field was that of Alfvén[1] where he studied the motion of a charged particle in an inhomogeneous electromagnetic field. This and subsequent study[2–4] have led to the recognition that instead of the random walk, the guiding center performs a slow adiabatic drift along some well defined contours. The attention to this problem was stimulated by its plasma physics applications, and mostly the three-dimensional case was considered. Not so long ago, the extension to the two-dimensional case was proposed by several authors[5] motivated by the quantum Hall effect studies.[6] We will discuss the two-dimensional case from now on.

Conventionally, the drift approximation is applied to the regime where the magnetic fields are so strong that the cyclotron radius $R_c=v/\omega_c$ is smaller than the correlation length d of the random potential. In this case the guiding center performs a drift along the constant energy contours of the random potential. For the potential of a general type all such contours except one are closed loops and thus the mo-

tion is finite. The motion is infinite only when a guiding center happens to be on the so-called percolating contour.[5] If one takes the drift picture literally, and attempts to calculate the average diffusion coefficient, the result will be equal to zero because the percolating contour has a zero measure.

Certainly, it has been understood that the drift picture is only an approximation. Nevertheless, the diffusion coefficient should be significantly smaller than the Drude-Lorentz prediction (1.2). We will show that the diffusion coefficient is, in fact, *exponentially small*.

Comparing the transport properties in the two regimes described above, we see that the increase in the magnetic field drives the system from the essentially delocalized, chaotic regime to the regime where the motion is regular and the trajectories of the particles are localized. We call this phenomenon the ''classical localization.'' The classical localization occurs because of an extremely ineffective energy exchange between two degrees of freedom, the cyclotron motion, and the guiding center motion. Without such an exchange the guiding center is bound to a certain constant energy contour. At the same time, the energy exchange is suppressed because the two degrees of freedom have very different characteristic frequencies, the cyclotron frequency ω_c being much larger than the drift frequency ω_d. Naturally, the present problem is directly related to the problem of a nonconservation of adiabatic invariants. The latter is known to be exponentially small,[7] and therefore it is not so surprising that the diffusion coefficient turns out to be exponentially small as well.[8]

One of the quantities we calculate in this paper is the value B_c of the magnetic field where the diffusion gives in to the classical localization as B increases. A naive guess would be the field where $R_c = d$. Let us, however, compare ω_c and ω_d at such a field. We denote the amplitude of the random potential $U(\boldsymbol{r})$ by W. We will assume that the potential is weak, $W \ll E$, where $E = mv^2/2$ is the particle's energy. The characteristic drift velocity is $v_d \sim \nabla U/m\omega_c \sim W/m\omega_c d$, and the drift frequency $\omega_d \sim v_d/d \sim W/m\omega_c d^2$. Hence, the ratio γ of the two frequencies is

$$\gamma = \frac{\omega_d}{\omega_c} \sim \frac{W}{m\omega_c^2 d^2} \sim \frac{W}{E}\left(\frac{R_c}{d}\right)^2, \quad R_c \lesssim d. \tag{1.4}$$

We see that at the point where $R_c = d$, this ratio is of the order of $W/E \ll 1$. Surprisingly, the classical localization must first arise already when $R_c \gg d$. To understand what kind of drift takes place in this case one can use the averaging method. This method was extensively developed by Krylov, Bogolyubov, and Mitropolsky[9] and in application to the problem at hand by Kruskal.[3] In the spirit of this method, one has to imagine that the slowly moving guiding center is entirely ''frozen'' on the time scale of the cyclotron period. One then calculates the average potential

$$U_0(\rho_x, \rho_y) = \oint \frac{d\phi}{2\pi} U(\rho_x + R_c \cos\phi, \rho_y + R_c \sin\phi), \tag{1.5}$$

acting on the particle during one cyclotron rotation. According to the averaging method, the drift of the guiding center is performed along the constant energy contours of the averaged potential $U_0(\boldsymbol{\rho})$. This conclusion was previously reached by Laikhtman.[10] If $R_c \ll d$, then the averaged potential coincides with the bare one and so, in agreement with the previous studies, the drift is performed along the constant energy contours of the bare potential. However, if $R_c \gg d$, then U_0 differs from U. The averaging reduces the amplitude of the potential by a factor $\sqrt{R_c/d}$, which is the square root of the number of uncorrelated ''cells'' of size d along the cyclotron orbit of length $2\pi R_c$. Hence, U_0 has the amplitude $W_0 \sim W\sqrt{d/R_c}$.

Now we can find the true boundary B_c of the classical localization. To this end we have to replace W by W_0 in Eq. (1.4), which gives

$$\gamma \sim \frac{W}{E}\left(\frac{R_c}{d}\right)^{3/2}, \quad R_c \gtrsim d, \tag{1.6}$$

and then solve $\gamma = 1$ for B. The result is

$$B_c = \frac{\sqrt{mc^2 E}}{ed}\left(\frac{W}{E}\right)^{2/3}. \tag{1.7}$$

The change of the transport regime at such field was predicted earlier by Baskin *et al.*[11] and by Laikhtman.[10] These authors noted that the displacement δr of the guiding center after one cyclotron period is a decreasing function of the magnetic field, $\delta r \sim \gamma d$ in our notations. Thus, at $B > B_c$ where $\gamma < 1$, such a displacement is smaller than the correlation length of the random potential. As a result, the scattering by the potential is no longer a sequence of uncorrelated acts and the motion of the guiding center is different from the random walk, which invalidates Eq. (1.2).

Although the crossover point B_c has been identified correctly, the understanding of the transport regime at larger magnetic fields remained not entirely satisfactory. For example, Baskin *et al.*[11] arrived at a strange conclusion that at $B > B_c$ the diffusion coefficient becomes larger than that given by Drude-Lorentz formula (1.2). On the other hand, the calculation of Laikhtman[10] relies on the existence of the random inelastic scattering processes. In this paper we address the question of *zero*-temperature transport where all the scattering acts are due to the static random potential only.

The key point of our approach is that the drift picture is albeit excellent but an approximation. A more accurate analysis given in Sec. II reveals that the diffusive motion is not restricted to the very percolating contour but persists within an area of finite width, so-called stochastic layer,[12] surrounding this contour. Such a layer turns out to be exponentially narrow if the magnetic field is larger than B_c. As a result, the phase-space averaged diffusion coefficient D is also exponentially small,

$$D \sim \omega_c d^2 e^{-B/B_c}. \tag{1.8}$$

Thus, the ''classical localization'' above B_c causes strong deviations from the conventional Drude-Lorentz formula (1.2).

The existence of the stochastic layer around the percolating contour is quite natural. Indeed, the classical localization is owing to the fact that drift trajectories are closed loops. It turns out that the drift along the loops passing sufficiently close to the saddle points of the random potential is unstable.

The instability is realized as a slow diffusion of the guiding center in the direction transverse to the drift velocity. Suppose that the percolation level is $U_0=0$. By virtue of a small transverse displacement, the particle drifting along the contour $U_0=-\epsilon$ can move to another closed contour $U_0=+\epsilon$. Although this displacement may be small, it will, in fact, lead to a much larger displacement at a later time because the center of the other loop is typically located a large distance away. Eventually, the particle can travel infinitely far from its initial position. This is the nature of the diffusion mechanism inside the stochastic layer.

The suppression of chaotic motion with increasing magnetic field proceeds as follows. At $B<B_c$ the chaotic motion takes place in the majority of the phase space, while the regular motion is restricted to small stability islands.[12] In this regime the correlations among the scattering acts can be ignored and Eq. (1.1) applies. As the magnetic field increases, the regions of regular motion expand while the stochastic layer shrinks. Above B_c the width of the stochastic layer starts to decrease exponentially leading to formula (1.8).

So far, we have discussed a purely classical dynamics. One can also study the transport properties of a noninteracting electron system quantum mechanically. Due to quantum interference, the conductivity of such a system turns out to be length-scale dependent.[15] The knowledge of classical dynamics enables one to find ''classical'' σ_{xx}, i.e., the conductivity, which would be measured on not too large length scales where effects of quantum interference are weak. Classical σ_{xx} is calculated as a product of the classical diffusion coefficient D and the quantum density of states $m/\pi\hbar^2$ (exponentially small de Haas–van Alphen oscillations being neglected). It is given by Drude-Lorentz formula (1.1) at $B<B_c$. At $B\sim B_c$ classical σ_{xx} reaches a value of $(e^2/h)G$, where

$$G=k_F d\left(\frac{W}{E}\right)^{2/3}, \tag{1.9}$$

$k_F=(1/\hbar)\sqrt{2mE}$ being the Fermi wave vector (E has the meaning of the Fermi energy). Finally, at $B>B_c$ classical σ_{xx} is given by

$$\sigma_{xx}\sim\frac{e^2}{h}Ge^{-B/B_c}. \tag{1.10}$$

Strictly speaking, the correct preexponential factor in this formula is not just G but a power-law function of B. We neglect this weaker dependence on the background of the overall exponential decrease of classical σ_{xx}. The sketch of classical σ_{xx} as a function of B is given in Fig. 1. As one can see, classical σ_{xx} quickly drops above $B=B_c$. In Fig. 1 we indicated one special value of the magnetic field, B_*, at which classical σ_{xx} reaches e^2/h,

$$B_*=B_c\ln G. \tag{1.11}$$

Here we assume that $G\gg 1$, i.e., that

$$d\gg k_F^{-1}\left(\frac{E}{W}\right)^{2/3}. \tag{1.12}$$

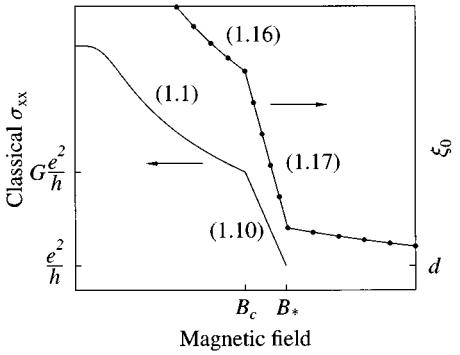

FIG. 1. Classical conductivity σ_{xx} (solid line) and the localization length ξ_0 (solid line with dots) at the *QHE conductivity minima* as functions of the magnetic field (schematically). Dots serve as a reminder that ξ_0 is defined at discrete values of the magnetic field. The curves are labeled by the equation numbers, which render their functional form in the corresponding intervals.

As we will see below magnetic field B_* plays an important role in the quantum transport.

At this point we would like to remind the reader that the true σ_{xx}, i.e., the one which is measured experimentally, is the conductivity on a large length scale (of the order of the sample size). The calculation of this quantity is much more difficult. Similar to the classical transport theory, there exist two mutually contradicting approaches. One is the theory of the Shubnikov–de Haas (SdH) effect, which aspires to predict the behavior of σ_{xx} in weak magnetic fields. The other is the theory of the quantum Hall effect (QHE), which is conventionally applied to strong fields.

At present, the transition from the SdH regime to the QHE is not well understood even for a noninteracting system. The traditional explanation of the QHE is based on the idea of localization; viz., it is believed that at zero temperature an electron can propagate diffusively only if its energy is precisely at the center of a Landau level (in strong fields).[6] This leads to isolated peaks in σ_{xx}, which are the signature of the QHE. On the other hand, in the theory of the SdH effect,[13,14] the suppression of σ_{xx} is related merely to the dips in the density of states between neighboring Landau levels, while the idea of localization is totally discarded. This crucial difference leads to different predictions for the conductivity minima. Arguing from the QHE standpoint, one expects zero dissipative conductivity, whereas the theory of SdH effect predicts a finite one.

In this paper we will advocate the following way to resolve this apparent contradiction. We will argue that at the QHE conductivity minima the states at the Fermi level are localized. At $B<B_*$ where B_* is given by Eq. (1.11), the localization length ξ_0 of such states is *exponentially large* but decreases from one minima to the next as B increases. Above B_c the falloff of ξ_0 is extremely sharp and at $B\simeq B_*$, which is only logarithmically larger than B_c, the localization length ceases to be exponentially large. Consequently, $B=B_*$ is the smallest magnetic field at which the observability of the QHE does not require *exponentially small* temperatures. This fact motivates us to identify the field $B=B_*$ as the starting point of the QHE. In other words, this is the position of the ''first'' QHE plateau.

To avoid confusion let us further elaborate on this issue.

Precisely at zero temperature one will observe the QHE peaks. Between the peaks σ_{xx} will be exactly zero because of the quantum localization. At finite temperature $T>0$ inelastic processes appear, which break the quantum coherence on length scales exceeding some temperature-dependent length $L_\phi(T)$. Thus, if $\xi_0>L_\phi(T)$, then the quantum localization is not important and the QHE features disappear. It is believed that the dependence of L_ϕ on T is some power law.[16] Therefore, if ξ_0 is exponentially large, then the inequality $\xi_0>L_\phi(T)$ is met already at exponentially small temperatures.

There is yet another way to see why the observability of the QHE requires small T when ξ_0 is large. It is known from experiment (see the bibliography of Ref. 17) that the low-temperature magnetotransport data at the σ_{xx} minima is consistent with the law

$$\sigma_{xx}\propto e^{-\sqrt{T_0/T}}, \tag{1.13}$$

which can be interpreted[17] in terms of the variable-range hopping in the presence of the Coulomb gap.[18] In this theory T_0 is directly related to ξ_0,

$$T_0=\text{const}\,\frac{e^2}{\kappa\xi_0}, \tag{1.14}$$

where κ is the dielectric constant of the medium. Deep minima of σ_{xx} are observable only if $T\ll T_0$. Thus, if ξ_0 is exponentially large, then the QHE can be observed only at exponentially small T. So, we reiterate once more that in practical terms there exists a starting point of the QHE. The precipitous drop of $\xi_0(B)$ above B_c leaves only a minimal ambiguity in identifying this point with $B=B_*$.

Our calculation of the localization length ξ_0 at the QHE minima of σ_{xx} is based on the following *ansatz*,[16,19] which we discuss in more detail in Sec. IV,

$$\xi_0\propto\exp(\pi^2 g_0^2), \quad g_0\gg 1. \tag{1.15}$$

Here $g_0=(h/e^2)\sigma_{xx}$ is the dimensionless classical conductance. Substituting Eqs. (1.1) and (1.10) into formula (1.15), we immediately find

$$\xi_0\propto\exp\left(G^2\frac{B_c^4}{B^4}\right), \quad B_c(W/E)^{4/3}<B<B_c, \tag{1.16}$$

$$\xi_0\propto\exp(G^2 e^{-2B/B_c}), \quad B_c<B<B_*. \tag{1.17}$$

The low-field end of the interval in Eq. (1.16) corresponds to $\omega_c\tau\sim 1$.

As one can see from Eqs. (1.16) and (1.17), the localization length indeed drops precipitously above $B=B_c$. At $B=B_*$, which is only logarithmically larger than B_c, g_0 becomes of the order of unity and ξ_0 ceases to be exponentially large. The dependence of ξ_0 on B in the interval $B_c(W/E)^{4/3}<B<B_*$ is illustrated by Fig. 1. The dependence of ξ_0 on B at even stronger magnetic fields, $B>B_*$, will be discussed in a forthcoming paper. At this point we can only say that at such fields the localization length is determined mainly by quantum tunneling and exhibits a power-law dependence on B.

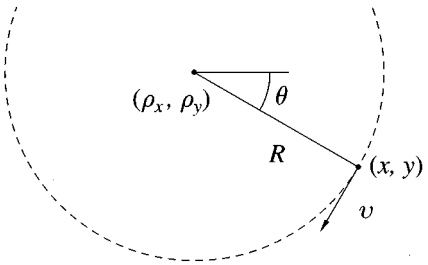

FIG. 2. The guiding center and cyclotron motion coordinates.

In order to verify our predictions concerning $\xi_0(B)$ experimentally, one has to measure σ_{xx} at very low temperatures and fit the data to the form (1.13). From such a fit one can deduce T_0, which is directly related to ξ_0 by virtue of Eq. (1.14).

The paper is organized as follows. In Sec. II we discuss the classical dynamics in strong ($B\gg B_c$) magnetic fields and demonstrate that the diffusion coefficient is exponentially small. In Sec. III we analyze the same problem from the quantum-mechanical point of view. Section IV is devoted to the derivation of Eqs. (1.16) and (1.17). Finally, in Sec. V we summarize our findings and discuss their relation to the experiment.

II. CLASSICAL DYNAMICS AT $B\gg B_c$

In this section we study the classical dynamics of a system with the Hamiltonian

$$H=\frac{\left(\boldsymbol{p}+\frac{e}{c}\boldsymbol{A}\right)^2}{2m}+U(\boldsymbol{r}), \quad \boldsymbol{A}=(0,-Bx,0). \tag{2.1}$$

It corresponds to a particle with negative charge $-e$ and the magnetic field in the negative $\hat{z}$ direction. Thus, the cyclotron gyration is clockwise. By means of the canonical transformation with the generating function

$$F(x,y,\theta,\rho_y)=m\omega_c\left[x(y-\rho_y)+\frac{(y-\rho_y)^2}{2}\cot\theta\right],$$

we obtain new momenta $-\partial F/\partial\rho_y=m\omega_c\rho_x$ and $-\partial F/\partial\theta\equiv I$. In terms of the new variables, the Hamiltonian (2.1) acquires the following form:

$$H=I\omega_c+U(\rho_x+R\cos\theta,\rho_y-R\sin\theta), \quad R\equiv\sqrt{\frac{2I}{m\omega_c}}. \tag{2.2}$$

It is easy to see that the pair (ρ_x,ρ_y) matches the earlier definition (1.3) of the guiding center coordinates. The geometrical meaning of the other variables is illustrated by Fig. 2.

The equations of motion are

$$\dot{\rho}_x=-\frac{1}{m\omega_c}\frac{\partial U}{\partial\rho_y}, \quad \dot{\rho}_y=\frac{1}{m\omega_c}\frac{\partial U}{\partial\rho_x}, \tag{2.3}$$

$$\dot{\theta}=\omega_c+\frac{\partial U}{\partial I},\quad \dot{I}=-\frac{\partial U}{\partial \theta}. \tag{2.4}$$

This system contains four dynamical variables, which makes its solution difficult. We can eliminate one of the variables, e.g., I, using the energy conservation. To this end we need to solve the equation

$$E=I\omega_c+U(\boldsymbol{\rho},\theta,I)$$

for I, or equivalently, the equation

$$R^2=\frac{2}{m\omega_c^2}[E-U(\boldsymbol{\rho},\theta,R)]$$

for R. For the potential U of an arbitrary strength this can be quite cumbersome. However, at least when the amplitude W of potential U is small enough,

$$W\ll E\frac{d}{R}, \tag{2.5}$$

it is sufficient to use an approximate solution

$$R\simeq R_c\equiv\sqrt{\frac{2E}{m\omega_c^2}}.$$

Condition (2.5) guarantees that the deviation of R from R_c is much smaller than the correlation length d of potential U. Under this condition we can also neglect the deviation of $\dot{\theta}$ from ω_c. As a result, Eqs. (2.3) and (2.4) can be treated as the equations of motion for the time-dependent Hamiltonian

$$H=U(\rho_x+R_c\cos\omega_c t,\rho_x-R_c\sin\omega_c t), \tag{2.6}$$

with ρ_y being the canonical coordinate and $m\omega_c\rho_x$ being the canonical momentum. It is customary to classify the systems of this kind as systems with $1\frac{1}{2}$ degrees of freedom.

It is useful to expand Hamiltonian (2.6) in the Fourier series,

$$H=\sum_k U_k(\boldsymbol{\rho})e^{-ik\omega_c t}, \tag{2.7}$$

with the expansion coefficients given by

$$U_k(\boldsymbol{\rho})\equiv\oint\frac{d\phi}{2\pi}U(\rho_x+R_c\cos\phi,\rho_y+R_c\sin\phi)e^{-ik\phi}, \tag{2.8}$$

[compare with Eq. (1.5)]. The new equation of motion for ρ_x is

$$\dot{\rho}_x=-\frac{1}{m\omega_c}\frac{\partial U_0}{\partial\rho_y}-\frac{1}{m\omega_c}\sum_{k\neq 0}\frac{\partial U_k}{\partial\rho_y}e^{-ik\omega_c t}, \tag{2.9}$$

and similarly for $\dot{\rho}_y$. If we drop the sum on the right-hand side of Eq. (2.9), then the remaining term will describe the drift of the guiding center along the contours of constant U_0. The local drift velocity $\boldsymbol{v}_d(\boldsymbol{\rho})$ is given by

$$\boldsymbol{v}_d(\boldsymbol{\rho})=\frac{1}{m\omega_c}\left(-\frac{\partial U_0}{\partial\rho_y},\frac{\partial U_0}{\partial\rho_x}\right). \tag{2.10}$$

Such a drift leads to the classical localization described in the previous section. The characteristic drift frequency is of the order of $\omega_d\sim W_0/m\omega_c d^2$, where W_0 is the amplitude of U_0 (see Sec. I). If the parameter $\gamma=\omega_d/\omega_c$ is small, then all the terms in the sum on the right-hand side Eq. (2.9) have frequencies much larger than the ω_d. They can be considered a high-frequency perturbation imposed on the ''unperturbed'' drift motion.

The presence of a small parameter calls for the perturbation theory treatment (averaging method) developed in Refs. 2–4. Unfortunately, it is not possible to calculate the diffusion coefficient perturbatively.[12,23] The calculation of the diffusion coefficient requires a different approach based on the consideration of the chaotic dynamics of the system within a narrow stochastic web surrounding the percolating contour of potential $U_0(\boldsymbol{\rho})$.

Due to an extreme difficulty of the problem, we restrict our consideration by two particular examples: a chessboard potential and a Gaussian random potential.

A. Chessboard geometry

Consider a chessboard potential

$$U(x,y)=-W\left(\cos\frac{x}{d}+\cos\frac{y}{d}\right).$$

In this case U_0 is given by

$$U_0=-W\mathcal{J}_0(R_c/d)\left(\cos\frac{\rho_x}{d}+\cos\frac{\rho_y}{d}\right). \tag{2.11}$$

More generally,

$$U_k=-W\mathcal{J}_k\left(\frac{R_c}{d}\right)\begin{cases} i^k\cos\dfrac{\rho_x}{d}+\cos\dfrac{\rho_y}{d}, & \text{even } k\\ i\left(i^k\sin\dfrac{\rho_x}{d}+\sin\dfrac{\rho_y}{d}\right), & \text{odd } k,\end{cases}$$

where $\mathcal{J}_k$'s are the Bessel functions.

As explained above, one can introduce the dimensionless parameter γ, which governs the classical dynamics. Equation (2.11) suggests that the appropriate definition for γ is

$$\gamma=\frac{W}{m\omega_c^2 d^2}|\mathcal{J}_0(R_c/d)|.$$

Note that with this definition γ vanishes whenever R_c/d coincides with a zero of $\mathcal{J}_0$. This property is a peculiarity of the periodic geometry. It leads to oscillations in the diffusion coefficient with the magnetic field, which are well known to exist both from theory and from experiment.[20,21] This behavior is nonuniversal and is not of primary interest to us. In the following we will assume that the ratio R_c/d is always close to midpoints between the successive zeros of $\mathcal{J}_0$. In this case, the dependence of γ on R_c is given by Eqs. (1.4) and (1.6). We will focus on the case $\gamma\ll 1$.

The ''unperturbed'' motion is described by the Hamiltonian

$$H_0=U_0(\boldsymbol{\rho}),$$

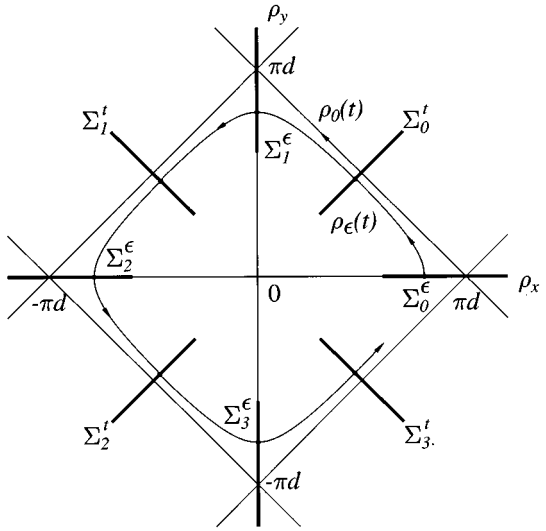

FIG. 3. A sketch illustrating the construction of the separatrix map. Two unperturbed orbits, $\boldsymbol{\rho}_0(t)$ and $\boldsymbol{\rho}_\epsilon(t)$ are shown. They follow two constant energy contours, $U_0=0$ (the separatrix) and $U_0=\epsilon<0$, respectively. The energy-time coordinates ϵ_n and t_n are defined by the crossings of the trajectories with the surfaces of section Σ_q^ϵ and Σ_q^t (shown by bold segments).

which is time independent. Hence, U_0 is the integral of motion in agreement with the statement that the drift is performed along the contours $U_0=\text{const}$. The motion has a periodic array of hyperbolic (or saddle) points. Some of them, $(\pi d,0)$, $(0,\pi d)$, $(-\pi d,0)$, $(0,-\pi d)$ are shown in Fig. 3, the others can be obtained by periodic translations. The hyperbolic points are connected by heteroclinic orbits or separatrices. One of them, which runs from $(\pi d,0)$ to $(0,\pi d)$ is shown in Fig. 3. It has the following time dependence:

$$\rho_y=2d\arctan e^{\gamma\omega_c(t-t_0)}, \quad \rho_x=\pi d-\rho_y, \tag{2.12}$$

where t_0 is the moment of crossing the surface of section Σ_0^t (see Fig. 3). The heteroclinic orbits passing through the other ''time surfaces'' Σ_q^t (see Fig. 3) have a similar functional form and an analogous dependence on the crossing times t_n's.

As explained in the Introduction, the unperturbed separatrix is dressed with a narrow stochastic layer. In the case of the chessboard potential, this layer has a topology of a square network. We are interested in the long-time asymptotic behavior of the chaotic transport along this network. An efficient tool to study such a transport is the separatrix map.[22,23] The separatrix map is an approximate map describing the dynamics near the separatrix. The application of the separatrix map to transport problems has been previously considered in Refs. 24–28.

To construct the separatrix map we will consider ''energy surfaces'' Σ_q^ϵ in addition to the introduced above time surfaces Σ_q^t. To avoid confusion we will elaborate a bit on the definition of such surfaces. Σ_q^ϵ's and Σ_q^t's are introduced for each chessboard cell. Index q runs from 0 to 3. The energy surfaces come through the saddle points and the time surfaces are drawn through the links connecting the neighboring saddle points. The locations of Σ_q^ϵ's and Σ_q^t's near the perimeter of the cell at the origin are clear from Fig. 3. The locations of the surfaces of section in the other cells can be obtained by periodic translations. Thus, index q in Σ_q^t refers to the position of the corresponding link with respect to a given cell's center. Similarly, index q in Σ_q^ϵ refers to the position of the saddle point.

Let $\boldsymbol{\rho}(t)$ be the exact trajectory near the separatrix. As t increases, $\boldsymbol{\rho}(t)$ crosses the surfaces Σ_q^ϵ in certain order. We denote by q_n the index of Σ_q^ϵ at nth crossing and by ϵ_n the value of U_0 at this moment. Due to the time-dependent terms in the Hamiltonian, ϵ_n changes with n. Let us find the difference $\epsilon_{n+1}-\epsilon_n$. The time derivative of U_0 is given by

$$\frac{dU_0}{dt}=-\sum_{k\neq 0}(\boldsymbol{v}_d\nabla U_k)[\boldsymbol{\rho}(t)]e^{-ik\omega_c t},$$

where $\boldsymbol{v}_d$ is the drift velocity, see Eq. (2.10). Notation $\boldsymbol{\rho}(t)$ stands for the exact trajectory, which is not known. Following Refs. 12,22,23, we perform the following approximations. First we replace the exact trajectory by the unperturbed one with $U_0=\epsilon_n$. Second, having in mind that $|\epsilon_n|\ll W_0$, we replace the trajectory with $U_0=\epsilon_n$ by the separatrix motion $\boldsymbol{\rho}_0(t-t_n)$, where $\boldsymbol{\rho}_0(t)$ is given by equations similar to Eq. (2.12) and t_n is the moment of time when $\boldsymbol{\rho}(t)$ crosses the surface of section $\Sigma_{q_n}^t$. As a result, we find

$$\epsilon_{n+1}-\epsilon_n=M_n(t_n), \tag{2.13}$$

where M_n is given by

$$M_n(t)=-\sum_{k\neq 0}\Delta_k(t), \tag{2.14}$$

$$\Delta_k(t)\equiv\int_{-\infty}^{\infty}dt'(\boldsymbol{v}_d\boldsymbol{\nabla}U_k)[\boldsymbol{\rho}_0(t'-t)]e^{-ik\omega_c t'}, \tag{2.15}$$

and is termed the Melnikov function.[29] It can be shown that the Δ_1 and Δ_{-1} yield the dominant contribution to M_n. After some algebra, the sum of these two terms acquires the form

$$M_n(t)\simeq 2\gamma\omega_c W\ \mathrm{Re}\int_{-\infty}^{\infty}dt'\frac{\tanh[\gamma\omega_c(t'-t)]}{\cosh[\gamma\omega_c(t'-t)]}\times\mathcal{J}_1(R_c/d)\exp\left(-i\omega_c t'+\frac{\pi}{4}+\frac{\pi q_n}{2}\right). \tag{2.16}$$

The integral can be evaluated by shifting the integration path to the complex plane of t. Then $M_n(t)$ can be represented by the sum of residues at the poles of the integrand. The residues from the poles closest to the real axis dominate the sum. Retaining only these terms, we arrive at

$$M_n(t)\simeq\Delta\epsilon\ \sin\vartheta_n, \tag{2.17}$$

$$\Delta\epsilon=4\sqrt{2}\pi m\omega_c^2 d^2\frac{\mathcal{J}_1(R_c/d)}{\mathcal{J}_0(R_c/d)}e^{-\pi/2\gamma}, \tag{2.18}$$

$$\vartheta_n=\omega_c t_n+\frac{\pi}{4}+\frac{\pi q_n}{2}. \tag{2.19}$$

Combining formulas (2.13) and (2.17), we obtain the first equation of the separatrix mapping

$$\epsilon_{n+1}=\epsilon_n+\Delta\epsilon\,\sin\,\vartheta_n. \tag{2.20}$$

To have the mapping in a closed form we need another equation relating t_{n+1} to t_n and ϵ_n. Following Refs. 12,22,23, we take

$$t_{n+1}=t_n+\frac{1}{4}T(\epsilon_{n+1}), \tag{2.21}$$

where $T(\epsilon)$ is the period of the unperturbed orbit $U_0(\boldsymbol{\rho})=\epsilon$. A straightforward computation gives

$$\frac{T(\epsilon)}{4}=\frac{1}{\gamma\omega_c}K\left(1-\frac{\epsilon^2}{4W_0^2}\right)\simeq\frac{1}{\gamma\omega_c}\ln\left|\frac{8W_0}{\epsilon}\right|,\quad |\epsilon|\ll W_0, \tag{2.22}$$

K being the complete elliptic integral of the first kind.

Although it is a common practice[12,22–29] to make the approximations similar to those we made above, their validity is far from being obvious. The justification has come only recently with a development by Treschev.[30]

Using his method, it is quite easy to show that the naive calculation of the Melnikov function is correct for $R_c\ll d$, where $|\mathcal{J}_k(R_c/d)|\ll|\mathcal{J}_0(R_c/d)|$ for all $k>0$. On the other hand, if $R_c\gg d$, then there is a large number of k, $k\lesssim R_c/d$, such that $\mathcal{J}_k(R_c/d)$ is of the same order of magnitude as $\mathcal{J}_0(R_c/d)$. In this case the straightforward application of Treschev's method is not an easy task. In this respect, our problem is much more complicated than the two model problems treated by Treschev.[30] However, the results obtained from the model problems strongly suggest that the right-hand side of Eq. (2.18) may be modified by at most a numerical factor. To summarize, in Eq. (2.18) the replacement

$$\frac{\mathcal{J}_1(R_c/d)}{\mathcal{J}_0(R_c/d)}\to j(R_c/d) \tag{2.23}$$

is needed. Without tedious calculations we can only say that function $j(x)$ tends to one in the limit $x\to 0$ while it remains of the order of one at $0<x<\infty$.

In addition to analytical work, the validity of the separatrix map has been investigated numerically by several authors[23,28] and has been rated from ''satisfactory'' to ''excellent.'' In the rest of this subsection we will assume that this is the case and calculate two quantities relevant for the transport, the width $\Delta\epsilon_{\rm web}$ of the stochastic layer around the separatrix and the average diffusion coefficient D.

The stochastic layer width $\Delta\epsilon_{\rm web}$ can be defined as the largest deviation of U_0 from zero found on the bundle of chaotic trajectories, which surround the destroyed unperturbed separatrix $U_0=0$. We estimate $\Delta\epsilon_{\rm web}$ following Ref. 23. First, we note that the relative change in ϵ_n after one application of the separatrix map is small provided $|\epsilon_n|\gg\Delta\epsilon$. Under this condition Eq. (2.21) can be linearized and then the map can be cast into the form of the standard map.[23] The standard map is characterized by a dimensionless parameter,

$$\mathcal{K}\equiv\frac{1}{\cos\,\vartheta_n}\left(\frac{\partial\vartheta_{n+1}}{\partial\vartheta_n}-1\right). \tag{2.24}$$

In our case $\mathcal{K}$ is given by

$$\mathcal{K}=\frac{\omega_c\Delta\epsilon}{4}\frac{dT(\epsilon_n)}{d\epsilon_n}=-\frac{\Delta\epsilon}{\gamma\epsilon_n}. \tag{2.25}$$

The crossover to the global stochasticity in the standard map occurs at $|\mathcal{K}|\simeq 0.97$ (Ref. 31), which yields the estimate

$$\Delta\epsilon_{\rm web}\simeq 18j(R_c/d)\frac{m\omega_c^2d^2}{\gamma}e^{-\pi/2\gamma} \tag{2.26}$$

for the stochastic layer's width. Note that $\Delta\epsilon_{\rm web}\sim\Delta\epsilon/\gamma$ is much larger than $\Delta\epsilon$, and so the approximation by the standard map is justified.

Let us now turn to the evaluation of the diffusion coefficient D. For the chessboard geometry this problem has been considered previously by Ahn and Kim.[28] Unfortunately, they calculated the diffusion coefficient averaged only over the trajectories inside the stochastic layer. We, however, are interested in the diffusion coefficient averaged over the *entire* phase space. Our approach to calculating D is close in spirit to the ones used for calculation of the diffusion coefficient in planar periodic vortical flows, e.g., Rayleigh-Bénard cells.[32,33] The details of the calculation can be found in Appendix A. The result is

$$D=0.45\frac{\Delta\epsilon}{m\omega_c}. \tag{2.27}$$

With the help of Eqs. (2.18) and (2.23) this translates into

$$D=7.9j(R_c/d)\omega_cd^2e^{-\pi/2\gamma}. \tag{2.28}$$

One may question the usefulness of the numerical factor in this formula on the grounds that function $j(x)$ is not known anyway. In regard of this we can say that first, the calculation of this numerical factor (Appendix A) and the calculation of $j(x)$ are two separate problems. Therefore, as soon as someone finds $j(x)$ using, say, Treschev's method,[30] Eq. (2.28) will yield the diffusion coefficient with no extra work. Second, our calculation demonstrates a close connection of the problem at hand with problems from a different field of physics, the fluid dynamics.

If the numerical factor is not desired, then D can be obtained from following simple arguments. Consider an ensemble of particles moving in the chessboard potential. Their diffusive motion can be visualized as a random walk from one chessboard cell to the next. The motion of each particle is a combination of the drift along the cell perimeter and the series of random displacements in the transverse direction. The rate of diffusion depends on the distance of a particle from the cell boundaries. The particles located within a distance of one transverse step from the cell boundaries possess the fastest rate because they can cross to the neighboring cell after a single passage along the cell's side. Particles further away from the perimeter remain trapped within the same cell for much longer time. Hence, their diffusion rate is negligible. Naturally, we can consider a model with an ϵ-dependent diffusion coefficient $D(\epsilon)=\Theta(\Delta\epsilon-|\epsilon|)d_0^2/T(\epsilon)$, where $\Theta(x)$ is the step func-

tion and $d_0=\sqrt{2}\pi d$ is the length of the cell's side. The net diffusion coefficient can be obtained by averaging $D(\epsilon)$ over the phase space, i.e., over the area in coordinates (ρ_x,ρ_y),

$$D=\frac{1}{d_0^2}\int_0^{\Delta\epsilon} d\epsilon D(\epsilon)\frac{dS(\epsilon)}{d\epsilon},$$

where $S(\epsilon)$ is the area of the cell's region bounded by the contours $U_0=0$ and $U_0=\epsilon$. It is trivial to show that $dS(\epsilon)/d\epsilon=T(\epsilon)/m\omega_c$; therefore, $D=\Delta\epsilon/m\omega_c$, which reproduces Eq. (2.27) up to a numerical factor.

Finally, the diffusion coefficient can be written as a function of the magnetic field B,

$$\ln\left(\frac{D}{\omega_c d^2}\right)\sim-\left(\frac{B}{B_{\rm cb}}\right)^{3/2}, \tag{2.29}$$

where

$$B_{\rm cb}=\frac{2^{7/6}}{\pi}\frac{\sqrt{mc^2E}}{ed}\left(\frac{W}{E}\right)^{2/3}$$

[cf. Eq. (1.7)]. Formula (2.29) was derived assuming that $\gamma\ll 1$, i.e., that $B\gg B_{\rm cb}$. In addition, we assumed that $R_c\gg d$, which is equivalent to $B\ll B_{\rm cb}(E/W)^{2/3}$. As one can see, the dependence of D on B for the chessboard geometry is given by a squeezed exponential with the exponent 3/2. In the next subsection we treat a more general case of a Gaussian random potential. We will show that the squeezed exponential is replaced by a simple one as given by Eq. (1.8).

B. Gaussian random potential

A Gaussian random potential is fully specified by its two-point correlator $C(\boldsymbol{r}_1-\boldsymbol{r}_2)$,

$$C(\boldsymbol{r}_1-\boldsymbol{r}_2)=\langle U(\boldsymbol{r}_1)U(\boldsymbol{r}_2)\rangle,\quad C(0)\equiv W^2.$$

In many cases, it is also convenient to deal with the Fourier transforms of U, which have the following correlator:

$$\langle\tilde{U}(\boldsymbol{q}_1)\tilde{U}(\boldsymbol{q}_2)\rangle=(2\pi)^2\delta(\boldsymbol{q}_1+\boldsymbol{q}_2)\tilde{C}(\boldsymbol{q}_1)$$

(Fourier transforms are denoted by tildes). Given the function $C(\boldsymbol{r})$, we want to calculate the diffusion coefficient in strong magnetic fields. Similar to the case of the chessboard potential, let us first investigate the ''unperturbed'' motion, the drift along the contours $U_0(\boldsymbol{\rho})=$const. Clearly, $U_0(\boldsymbol{\rho})$ is also a Gaussian random potential with correlator C_0 related to C by

$$\tilde{C}_0(q)=[\mathcal{J}_0(qR_c)]^2\tilde{C}(q).$$

The unperturbed motion is determined by the properties of the level lines of U_0. It is known that all such lines except one, the percolating contour, are closed loops. The Gaussian random potential shares this property with the chessboard potential considered above. In addition, the position of the percolation level is the same for both potentials: $U_0=0$. There exists, however, an important difference in the properties of level lines in the two cases. The diameters of the loops in the chessboard do not exceed $2\pi d$. On the other hand, constant energy contours of the random potential can have arbitrarily large diameters. Such large loops are found in the vicinity of the percolating contour. (The latter one can be considered as a loop with infinitely large diameter.) As the diameter of the contour increases, the range of U_0 found at such contours shrinks, tending to the percolation level $U_0=0$.

Similar to the chessboard geometry case, the exact trajectories do not simply follow the level lines of $U_0(\boldsymbol{\rho})$ but exhibit small transverse deviations from them. As a result, a finite diffusion coefficient appears. As we will see below this diffusion coefficient is *much larger* than that for the chessboard potential of the same amplitude and correlation length. The reason for this difference comes from an important role of *rare places* where drift trajectories pass nearby unusually large maxima of U_0.

To calculate D we will use a close analogy of the problem at hand with the problem of calculating the effective diffusion constant of a particle diffusing in an incompressible flow.[34] Below we essentially reproduce the basic arguments of Isichenko *et al.*[34] with slight modifications appropriate for our problem.

Borrowing the terminology of Ref. 34, we call a bundle of constant U_0 contours with diameters between a and $2a$ a convection cell or an a cell (see Fig. 17 of Ref. 34). The values of U_0 in typical a cells belong to an interval $[-w(a),w(a)]$, which narrows with increasing a. Let us denote by $L(a)$ the perimeter length of typical a cells and by $\Delta\epsilon(a)$ the change in U_0 accumulated along the trajectory following the perimeter, for which the time $T(a)\sim L(a)/v_d$ is required. The key point in estimating D is a ramification between mixing [with $\Delta\epsilon(a)>w(a)$] and nonmixing [$\Delta\epsilon(a)<w(a)$] cells. It takes a single period $T(a)$ or even a fraction of thereof for the particle to leave a mixing cell, whereas particles in nonmixing cells remain trapped for time intervals much larger than $T(a)$. The dominant contribution to the transport comes from the mixing cells of the largest width $w(a)$ for which $\Delta\epsilon(a)\sim w(a)$. We denote the diameter by such cells by a_m. The particles situated in such cells perform a random walk from one optimal cell to the next. The characteristic step of the random walk is a_m and the characteristic rate of the steps is $1/T(a_m)$. Thus, the diffusion coefficient of such ''active'' particles is of the order of $a_m^2/T(a_m)$. The net diffusion coefficient can be found by multiplying this diffusion coefficient by the fraction of the total area occupied by the optimal convection cells. Note that the width of the a_m cells in the real space is of the order of $\Delta\epsilon(a_m)d/W_0$. Using this, the fraction of the area can be estimated to be $[\Delta\epsilon(a_m)d/W_0]L(a_m)/a_m^2=[\Delta\epsilon(a_m)/m\omega_c]T(a_m)/a_m^2$. Finally, we obtain

$$D\sim\frac{\Delta\epsilon(a_m)}{m\omega_c}, \tag{2.30}$$

which closely resembles Eq. (2.27) for the chessboard.[35] However, now $\Delta\epsilon_m\equiv\Delta\epsilon(a_m)$ depends on the diameter a_m of the optimal cells, which has yet to be found. We see that the calculation of D hinges upon the calculation of $\Delta\epsilon_m$. To accomplish the latter task we can make the same kind of approximations as in deriving the separatrix mapping for the chessboard. Then we obtain the following expression [cf. Eqs. (2.14) and (2.15)]:

$$\Delta\epsilon_m^2=\sum_{n\neq 0}|\Delta_n|^2, \tag{2.31}$$

$$\Delta_n\equiv\oint dt(\boldsymbol{v}_d\boldsymbol{\nabla}U_n)[\boldsymbol{\rho}_0(t)]e^{-in\omega_c t}, \tag{2.32}$$

where the integration path is the unperturbed orbit $U_0[\boldsymbol{\rho}_0(t)]=\text{const}$ belonging to a given a_m cell. Observe that the integrand is the product of a slowly changing function $f_n(t)=(\boldsymbol{v}_d\boldsymbol{\nabla}U_n)[\boldsymbol{\rho}_0(t)]$ and a rapidly oscillating exponential factor $e^{-in\omega_c t}$. It is customary to estimate such integrals by shifting the integration path into the lower half plane of complex t where the oscillating factor decays exponentially. By using the method, one arrives at the following estimate:

$$\Delta\epsilon_m^2\sim|\Delta_1|^2=\left|\sum_k 2\pi i R_k e^{-|\mathrm{Im}\ \tau_k|\omega_c}\right|^2, \tag{2.33}$$

where τ_k are the singular points of the function $f_1(t)$ in the lower half plane plane and R_k are some preexponential factors. For example, if $f_1(t)$ has a simple pole at τ_k, then R_k is up to a phase factor the residue of such a pole. Equation (2.33) is similar to Eqs. (2.17)–(2.19) for the chessboard potential.

We denote the coordinate along the drift trajectory by s, then $f_1(t)=v_d(dU_1/ds)$. The singularities of $f_1(t)$ may originate either from v_d or from (dU_1/ds). Let us investigate the former possibility. To get the necessary insight we will use the exactly solvable model of the chessboard potential, which we studied above. In the latter case

$$v_d(t)=\frac{\sqrt{2}\gamma\omega_c d}{\cosh[\gamma\omega_c(t-t_0)]} \tag{2.34}$$

[see Eq. (2.12)] and the singularities of $v_d(t)$ in the lower half plane consist of the ''parent'' pole at $t_0-i\pi/2\gamma\omega_c$ and a series of ''daughter'' poles at $t_0-i\pi(k+1/2)/\gamma\omega_c$, $k=1,2\ldots$. Note that the imaginary part of the parent pole is of the order of the characteristic time scale $(\gamma\omega_c)^{-1}$ of the drift motion.

In the case of the random potential, we also expect to find a series of singularities of $v_d(t)$. However, there will be not a single series but a large number $N(a_m)$ of them. Indeed, $v_d(t)$ has about $L(a_m)/d$ minima on the trajectory $s(t)$. The points of minima divide the trajectory into $L(a_m)/d$ intervals of length $\sim d$. In each interval $v_d(t)$ first rises, then reaches a maximum, then decreases, i.e., it exhibits the same kind of behavior as in the chessboard case. Therefore, a naive estimate of $N(a_m)$ is $N(a_m)\sim L(a_m)/d$. Since Im τ_k's enter Eq. (2.33) in the arguments of the exponentials, the dominant contribution to $\Delta\epsilon_m$ comes from these $N(a_m)$ parent singularities. Let us now discuss Im τ_k's. It is obvious that different a_m cells give rise to different Im τ_k's, i.e., there exists a certain distribution of Im τ_k's. What kind of distribution should we expect? Clearly, the *typical* value of the imaginary parts of the parent singular points should be of the order of the characteristic time scale of the drift motion, $(\gamma\omega_c)^{-1}$, where γ can be defined as follows:

$$\gamma=\frac{W_0}{m\omega_c^2 d^2},$$

with W_0 and d being

$$W_0=\sqrt{C_0(0)},\quad d=\sqrt{-\frac{C_0}{2\boldsymbol{\nabla}^2 C_0}}.$$

However, it would be a mistake to think that $\Delta\epsilon_m$ is determined by this typical value. Indeed, the deviations of Im τ_k from their average value are dramatically enhanced in $\Delta\epsilon_m$ due to a large value of ω_c compared to ω_d. Therefore, we can expect an extremely broad range of the exponential factors entering the sum on the right-hand side of Eq. (2.33). At the same time, there is no such enhancement for R_k. This kind of argument implies that we can estimate $\Delta\epsilon_m$ considering only the distribution of Im τ_k's, i.e.,

$$\Delta\epsilon_m^2\sim\left|\sum_k e^{i\vartheta_k}e^{-|\mathrm{Im}\ \tau_k|\omega_c}\right|^2,$$

where ϑ_k is the phase of the complex number R_k. We will further assume that ϑ_k's are uncorrelated, which results in

$$\Delta\epsilon_m^2\sim\sum_k e^{-2|\mathrm{Im}\ \tau_k|\omega_c}.$$

From this, we find that

$$\Delta\epsilon_m^2\sim W_0^2\frac{L(a_m)}{d}\int_0^\infty d\gamma' P(\gamma')e^{-2/\gamma'}, \tag{2.35}$$

where $\gamma'=1/\mathrm{Im}\ \tau\omega_c$ and $P(\gamma')$ is the distribution function of γ'. The first factor on the right-hand side is written solely to provide the correct dimensionality.

In general, $P(\gamma')$ depends on the functional form of $C(\boldsymbol{r})$. Suppose that $C(\boldsymbol{r})$ is isotropic, i.e., depends only on $r=\sqrt{x^2+y^2}$. It is possible to show that for $C(r)$ with ''good'' analytical properties, $P(\gamma')$ has the Gaussian tail,

$$P(\gamma')\sim\exp\left(-\frac{A\gamma'^2}{\gamma^2}\right),\quad \gamma'\gg\gamma, \tag{2.36}$$

where $A\sim 1$ is some number. The conditions for Eq. (2.36) to hold are as follows. Function $C(r)$ must be analytic for all real r. In addition, $C(r)$ must be analytic in some complex neighborhood of $r=0$. Note that such conditions can be met only if $\widetilde{C}(q)$ decays exponentially or faster at large q, e.g.,

$$\ln C(r)\sim-(qd)^\beta,\quad \beta\geq 1.$$

For example, a ''realistic'' potential defined by Eq. (B1) below corresponds to $\beta=1$ and therefore meets the requirements. In fact, we found the value of $A=5.0$ for potentials of this type. We omit the details of the calculation and the proof of Eq. (2.36) (Ref. 36) for the sake of keeping the size of the paper within the manageable limits. Instead, we chose to present simple physical arguments leading to Eq. (2.36).

Let us again examine the chessboard model. As one can see from Eq. (2.34), v_d as a function of t exhibits a brief pronounced pulse near its maximum at $t=t_0$. The duration of the pulse is of the order of $(\gamma\omega_c)^{-1}$. It is this time scale that determines the imaginary part of the closest singular point. Let us now return to the random potential case. One can speculate that singular points of $v_d(t)$ are always associated

with such kind of pulses. By this argument, the singularity at the point $t_s=t_1-it_2$ with $0<t_2\ll(\gamma\omega_c)^{-1}$ requires an unusually short pulse of duration $\Delta t\sim t_2$. To produce such a pulse $v_d(s)$ must have a large and sharp maximum. In other words, the gradient of U_0 must be untypically large at this point. Let us estimate, e.g., the height of the maximum in $v_d(s)$. The half width Δs of the maximum is of the order of $\Delta s\sim\sqrt{-v_d/v_d''}$. On the other hand, we should have $\Delta s\sim v_d t_2$. Thus, $v_d v_d''\sim -t_2^{-2}$, which shows that small values of Im t_s require large values of v_d and its second derivative, $v_d\sim d/t_2$ and $v_d''\sim 1/t_2 d$. Recall now that the distribution functions of both v_d and v_d'' have Gaussian tails, so that the probability of finding an unusually large v_d is of the order of $\exp(-A_1 v_d^2/\gamma^2\omega_c^2 d^2)$ and similarly for v_d'' ($A_1\sim 1$ is some number). Substituting $d/t_2\sim\gamma'\omega_c d$ for v_d, we arrive at Eq. (2.36).

The estimation of the integral in Eq. (2.35) by the saddle-point method results in

$$\Delta\epsilon_m^2\sim W_0^2\frac{L(a_m)}{d}\exp\left(-\frac{3A^{1/3}}{\gamma^{2/3}}\right). \tag{2.37}$$

On the other hand, $L(a_m)$ obeys the scaling law

$$L(a_m)\propto|\Delta\epsilon_m|^{-\nu d_h}, \tag{2.38}$$

where ν and d_h are some exponents, which depend on the properties of the correlator $\tilde{C}_0(q)$ (Ref. 34). Their actual values are not very important at this point. Equations (2.37) and (2.38) enable one to find $\Delta\epsilon_m$, which can then be substituted into Eq. (2.30). As a result, we find the diffusion coefficient,

$$D\sim\omega_c d^2\gamma^\alpha\exp\left(-\frac{J}{\gamma^{2/3}}\right), \tag{2.39}$$

where α is some number and

$$J=\frac{3A^{1/3}}{1+\nu d_h}$$

is another number. Strictly speaking, we cannot calculate the correct preexponential factor in formula (2.39). The particular choice of this factor made in Eq. (2.39) provides a matching of this equation with Drude-Lorentz formula (1.2) at $\gamma=1$ where both formulas give $D\sim\omega_c d^2$ (up to purely numerical factors). This can be seen from Eqs. (1.2), (1.6), and (2.39) if one takes into account the approximate expression[38] for the transport time τ,

$$\tau\sim\frac{d}{v}\left(\frac{E}{W}\right)^2.$$

In this subsection we implicitly assumed that the inequality $R_c\gg d$ holds. In this case $\gamma\propto B^{-3/2}$ [Eq. (1.6)]. Substituting this into Eq. (2.39), we obtain

$$D\propto\omega_c d^2 e^{-B/B_c},\quad B>B_c,$$

declared previously in Sec. I. The factor γ^α on the right-hand side is dropped under the assumption that in the interval $B_c<B<B_*$, discussed in Sec. I, this factor does not appreciably deviate from unity.

Concluding this section, we would like to point out that the dependence of D on the magnetic field is given by a simple exponential not the squeezed one as in the chessboard model [Eq. (2.29)]. The reason for this difference comes from the important role of rare places on the trajectories with unusually sharp features of the averaged potential U_0.[37]

III. INTER-LANDAU-LEVEL TRANSITION AMPLITUDES

In the preceeding section we showed that in strong magnetic fields, $B>B_c$, the guiding center of the cyclotron orbit closely follows the level lines $U_0=$const of the averaged potential U_0. A nonvanishing diffusion coefficient appears due to small deviations from the level lines. The characteristic value $\Delta\epsilon_m$ of such a deviation was calculated purely classically. Due to the energy conservation, $\Delta\epsilon_m$ also represents the change in the kinetic energy $I\omega_c$ of the particle [Eq. (2.2)].

The purpose of this section is to calculate the change in kinetic energy quantum mechanically by taking into account the discreetness of the spectrum, i.e., the existence of the Landau levels (LL's). Note that this is not yet a consistent quantum-mechanical treatment of the problem. For example, in this section we ignore localization and/or quantum tunneling. An attempt to touch on some of those complicated issues will be postponed until the next section.

In quantum-mechanical terms, the change in kinetic energy results from inter-LL transitions. Indeed, the change in kinetic energy due to $N\to N+k$ transition is equal to $k\hbar\omega_c$. We denote the transition amplitude upon the completion of the loop $U_0=$const by $A_{N,N+k}$, then $\langle\Delta\epsilon_m^2\rangle$ is given by

$$\langle\Delta\epsilon_m^2\rangle=(\hbar\omega_c)^2\sum_k k^2|A_{N,N+k}|^2. \tag{3.1}$$

It is obvious from this formula that the inter-LL transitions may be significant only within a certain band of LL's. If $\Delta\epsilon_m$ is larger than $\hbar\omega_c$, then the number of LL's in that band should be of the order of $\Delta\epsilon_m/\hbar\omega_c$. We denote by B_* the field where $\Delta\epsilon_m=\hbar\omega_c$. In fact, this notation has already been used in Sec. I [Eq. (1.11)]. If $B>B_*$, then $\Delta\epsilon_m<\hbar\omega_c$ and even the transitions to the neighboring LL's must be suppressed. In this case the sum over k is dominated by the two terms, $k=\pm 1$; therefore,

$$|A_{N,N\pm1}|^2=\frac{\langle\Delta\epsilon_m^2\rangle}{2(\hbar\omega_c)^2}. \tag{3.2}$$

In deriving Eqs. (3.1) and (3.2) we implicitly assumed that the classical and the quantum calculations of $\langle\Delta\epsilon_m^2\rangle$ give the same result. This will be demonstrated below.

Before we do so, let us mention one interesting fact. Using Eq. (2.30) and the Einstein relation $\sigma_{xx}=e^2\nu D$, where $\nu=m/\pi\hbar^2$ is the density of states (de Haas–van Alphen oscillations neglected), one arrives at the following formula:

$$\sigma_{xx} \sim \frac{e^2}{h} \frac{\Delta \epsilon_m}{\hbar \omega_c}.$$

It can be interpreted in the following way: the transport is determined by the aforementioned band of about $(\Delta \epsilon_m / \hbar \omega_c)$ LL's with energies near the Fermi energy. Each level contributes e^2/h to σ_{xx} (cf. Ref. 39).

The general formula for $A_{N,N+k}$ derived in Appendix C reads

$$A_{N,N+k} = \int_0^{2\pi} \frac{d\theta}{2\pi} e^{-ik\theta} \exp\left(-\sum_{n \neq 0} \frac{\Delta_n}{n \hbar \omega_c} e^{-in\theta} \right), \quad (3.3)$$

where Δ_n's are given by Eq. (2.32). Substituting this expression into formula (3.1) and taking advantage of the identity

$$\int_0^{2\pi} \frac{d\theta}{2\pi} \sum_{k=-\infty}^{\infty} k^2 e^{ik\theta} f(\theta) = -f''(0),$$

we recover the classical formula (2.31) for $\Delta \epsilon_m^2$.

Finally, it is easy to see that Eq. (3.2), which we derived without any calculations, is consistent with formula (3.3). Indeed, $|\Delta_1| \simeq \Delta \epsilon_m$. If $\Delta \epsilon_m \ll \hbar \omega_c$, then the second exponential in Eq. (3.3) can be expanded in the Taylor series, which trivially leads to Eq. (3.2).

IV. QUANTUM LOCALIZATION LENGTH

In Sec. I we argued that the localization length is exponentially large in weak magnetic fields and has to decay as the magnetic field increases. This statement is an oversimplification in two respects. First, ξ is, in fact, expected to diverge at certain discreet values B_N of the magnetic field

$$\xi = \xi_0 \left| \frac{B_{N+1} - B_N}{B - B_N} \right|^{\mu}, \quad (4.1)$$

where μ is a critical exponent.[6] Second, such divergences neglected, ξ starts decreasing only from $B \sim \hbar c / e l_{\rm tr}$, at which the magnetic length $l = \sqrt{\hbar / m \omega_c}$ becomes of the order of the transport length $l_{\rm tr} = v \tau$.

Let us discuss these issues in some detail. Scaling theory of localization is one possible way to approach this difficult problem.[15] In scaling theory one tries to understand the localization by considering the behavior of the dimensionless conductance $g \equiv (h/e^2) \sigma_{xx}$ as a function of system size L. This behavior is described by the scaling function

$$\beta(g) = \frac{\partial \ln g}{\partial \ln L}. \quad (4.2)$$

One starts with calculating the conductance $g_0 = g(l_0)$ at some short length scale $L = l_0$, where it is large and then finds how g is renormalized towards larger L. The localization length is the length scale where $g(L)$ becomes of the order of unity. (If g_0 is of the order of unity or smaller, then a different approach has to be used, see below.)

It has been conjectured[40] that all physical systems can be grouped into certain universality classes with the same functional form of the scaling function. If we neglect the spin-orbit coupling, then the appropriate universality class for our system is determined by the relation between L and the magnetic length l. For $L \ll l$, the system belongs to the orthogonal class, where the scaling function is given by[15,40]

$$\beta(g) \simeq -\frac{2}{\pi g}, \quad L \ll l. \quad (4.3)$$

For $L \gg l$ the system is in the unitary class. The scaling function is given by

$$\beta(g) \simeq -\frac{1}{2\pi^2 g^2}, \quad L \gg l. \quad (4.4)$$

The latter result was derived both by the conventional diagram technique[42,43] and by an effective field theory.[40] Solving the scaling equation (4.2) for $g(L)$, we find that ξ experiences a growth from the value of

$$\xi \sim l_{\rm tr} \exp\left(\frac{\pi}{2} k_F l_{\rm tr} \right) \quad (4.5)$$

at $B = 0$ to

$$\xi \sim l_{\rm tr} \exp(\pi^2 k_F^2 l_{\rm tr}^2) \quad (4.6)$$

at $B \sim \hbar c / e l_{\rm tr}^2$, where $l = l_{\rm tr}$. In stronger fields, $B > \hbar c / e l_{\rm tr}^2$, the system belongs to the unitary class at all relevant length scales and ξ is given by the formula[16,19]

$$\xi = l_0 \exp[\pi^2 g_0 (B)^2] \quad (4.7)$$

following from Eq. (4.4). The dimensionless conductance $g_0(B)$ decreases with B. For the case of a long-range random potential this follows from the results of the preceeding sections. Therefore, the initial *growth* of ξ at very weak magnetic fields is followed by the exponential *decay* of ξ as B increases. This is the statement we put forward in Sec. I.

Unfortunately, Eq. (4.7) cannot be entirely correct because it does not reproduce the critical divergences [Eq. (4.1)]. Pruisken[41] argued that the critical behavior is a nonperturbative effect. His field-theoretical treatment yields an expression for the β function, in principle, different from the simple form (4.4). However, the deviations from Eq. (4.4) become significant only when the renormalized value of g approaches unity. On this basis we speculate that Eq. (4.7) gives only the lower bound for the localization length ξ. We further assume that this lower bound is close to the actual value of ξ away from criticality. In other words, Eq. (4.7) gives, in fact, not ξ itself but its noncritical prefactor ξ_0 entering Eq. (4.1).

Note that $\xi \simeq \xi_0$ at the midpoints between neighboring divergences of ξ, i.e., at the QHE conductivity minima. This is exactly the quantity discussed in Sec. I where we postulated the *ansatz* (1.15) [the same as Eq. (4.7) but with ξ_0 instead of ξ]. By virtue of this *ansatz*, the calculation of ξ_0 boils down to the evaluation of the short length-scale conductance g_0.

Previous attempts[41–43] to treat the localization problem in the QHE have been focused on the case of a short-range random potential, i.e., the potential whose correlation length is much smaller than de Broglie wavelength $2\pi/k_F$. In this case g_0 has to be calculated quantum mechanically, e.g., within a self-consistent Born approximation.[13,14] Recall that our theory applies to the case $k_F d \gtrsim (E/W)^{2/3} \gg 1$, see Eq.

(1.12). Therefore, there is a whole intermediate region $1 \ll k_F d \ll (E/W)^{2/3}$ separating the domains of applicability of our and the previous theories. The calculation of ξ_0 in that region is a separate problem and will be discussed elsewhere.

In the case of long-range random potential, which we consider here, $g_0(B)$ can be calculated with the help of Einstein relation,

$$g_0(B) = h\nu(B)D(B),$$

where $\nu(B)$ is the density of states at the Fermi level and $D(B)$ is the classical diffusion coefficient. According to the results of the previous sections, $D(B)$ is given by Drude-Lorentz formula (1.2) at $B < B_c$ and by formula (2.39) at $B > B_c$. Let us now discuss the behavior of $\nu(B)$. In principle, $\nu(B)$ oscillates with B around its zero-field value $\nu(0) = m/\pi\hbar^2$. However, for B smaller or at least not to much larger than B_c such oscillations are exponentially small because the width of LL's, which is of the order of W_0 (Ref. 44), is much larger than the distance $\hbar\omega_c$ between them. Therefore, we can use the zero-field value $\nu(0)$.

Substituting all these results into Eq. (1.15), we obtain $\xi_0(B)$. The functional form of this dependence is given by Eqs. (1.16) and (1.17). Graphically, it is illustrated by Fig. 1. Observe that the overall decay of ξ_0 as B increases becomes extremely sharp at $B > B_c$. As a consequence, already at the field $B = B_*$, which is only logarithmically larger than B_c [see Eq. (1.7)], ξ_0 ceases to be exponentially large. At $B > B_*$, g_0 becomes less than one and Eq. (1.15) does not hold anymore. In this region the localization length is determined mainly by quantum tunneling rather than by the destructive interference of classical diffusion paths. Thus, the calculation of ξ_0 requires a different approach. It will be discussed in a forthcoming paper together with the prefactor in formula (1.17). At this point we can only say that ξ_0 is expected to have a power-law dependence on B and eventually match the predictions of Raikh and Shahbazyan[45] at sufficiently large B.

V. DISCUSSION AND CONCLUSIONS

In this paper we studied a two-dimensional motion of a charged particle in a weak long-range random potential and a perpendicular magnetic field. We showed that the phase-space averaged diffusion coefficient is given by Drude-Lorentz formula only at magnetic fields B smaller than certain value B_c. At larger fields, the chaotic motion is suppressed and the diffusion coefficient becomes exponentially small.

To make a connection with the experiment our results can be applied to the following model. We suppose that the random potential is created by randomly positioned ionized donors with two-dimensional density n_i set back from the two-dimensional electron gas by an undoped layer of width d. We will assume that $n_i d^2 \gg 1$ and also that $d \gg a_B$, where a_B is the effective Bohr radius. In this case the random potential can be considered a Gaussian random potential whose correlator is given in Appendix B. As a particular example, we consider a special case where the density of *randomly positioned* donors is equal to the density $k_F^2/(2\pi)$ of the electrons. We call it the standard potential. It is easy to see that for the standard potential $E/W \sim k_F d$ and the domain of applicability of our theory [Eq. (1.12)] is simply $k_F d \gg 1$. In modern high-mobility GaAs devices this parameter can be as large as ten. It is easy to verify that the magnetic field B_c where the classical localization takes place corresponds to the LL index $N_c \sim (k_F d)^{5/3}$, which can be a number between 10 and say, 50 for GaAs heterostructures. Another important magnetic field B_* [Eq. (1.11)] corresponds to LL index N_*, which is only slightly smaller than N_c. As explained in Sec. I, N_* is the number of the ''first'' QHE plateau in the sense that the observability of plateaus with larger N require *exponentially small* temperatures.

The point $N = N_*$ plays another important role. It is the largest N where it is possible to see the activated transport $\sigma_{xx} \propto e^{-E_a/T}$, $E_a \simeq \hbar\omega_c/2$ at the minima of σ_{xx}. Indeed, it is known that in strong fields or for small N's the dissipative conductivity demonstrates the Arrhenius-type behavior at not too low temperatures. As the temperature decreases, the activation becomes replaced by the variable-range hopping, see Eq. (1.13).

Equating the two exponentials, we find the temperature T_h at which the activation gives in to the hopping,

$$T_h \sim \frac{(\hbar\omega_c)^2}{T_0}. \tag{5.1}$$

This formula can also be written in another form,

$$\frac{T_h}{\hbar\omega_c} \sim \frac{\hbar\omega_c}{T_0} = \text{const}\,\frac{\xi_0}{r_s R_c}, \tag{5.2}$$

where $r_s = \sqrt{2}e^2/\kappa\hbar v_F$ is the gas parameter, which is of the order of unity in practice. Let us demonstrate that the activated behavior should not be observable at $B < B_*$. Indeed, it makes sense to talk about the activated behavior only at temperatures below the activation energy $E_a \simeq \hbar\omega_c/2$. Therefore, the activated transport can be observable only if the right-hand side of Eq. (5.2) is less than unity. Thus, the Arrhenius-type behavior of σ_{xx} cannot be detected in magnetic fields much smaller than B_* where ξ_0 is still exponentially large. On the other hand, it can be shown, and it is a subject of a forthcoming paper, that in the standard case the ratio $\xi_0(B_c)/R_c$ is smaller than one. Consequently, the point where the activated transport becomes observable for the first time with an increase in B is indeed the point $B \simeq B_*$.

The behavior of ξ_0 in magnetic fields stronger than B_* has not been investigated in the present paper. It will be discussed elsewhere. We expect that at such magnetic fields $\xi_0(B)$ is a certain power law matching the results of Raikh and Shahbazyan[45] at sufficiently large B. As explained in Sec. I, such a dependence can be studied experimentally.

Finally, in this paper we have neglected the influence of electron-electron interaction on ξ_0. This complicated issue warrants further study.

ACKNOWLEDGMENTS

We are grateful to A. P. Dmitriev, I. V. Gornyi, V. Yu. Kachorovskii, A. I. Larkin, and D. L. Shepelyansky for useful discussions and to A. A. Koulakov for a critical reading of the manuscript. This work is supported by NSF under

Grant No. DMR-9616880 and by the Russian Fund for Fundamental Research.

APPENDIX A: DIFFUSION COEFFICIENT IN THE CHESSBOARD MODEL

To calculate the numerical factor in Eq. (2.27) for the diffusion coefficient we proceed as follows. First, we will introduce the random-phase model[28] arguing as follows. The well-known property of the standard map is a fast mixing in the phase variable ϑ. The correlations in phase decay according to $\langle e^{i(\vartheta_n-\vartheta_0)}\rangle\sim|\mathcal{K}|^{-n/2}$ (Ref. 12) as a function of the iteration number n and the map parameter $\mathcal{K}$ [Eq. (2.24)]; therefore, for $|\mathcal{K}|\gg1$ the phase memory is typically lost after a single iteration of the map. The situation with the separatrix map is similar, which allows a simplification of the problem. We will assume that ϵ_n is still transformed according to Eq. (2.20) as long as $|\epsilon_{n+1}|\leqslant\Delta\epsilon_{\rm web}$. If the new value of $|\epsilon_{n+1}|$ is larger than $\Delta\epsilon_{\rm web}$, then $\epsilon_{n+1}=\epsilon_n$. At the same time, ϑ_n will be a purely random variable uniformly distributed in the interval $(0,2\pi)$. As we will see below, for transport only the narrow boundary layer $|\epsilon|\sim\Delta\epsilon$ is important (cf. Refs. 32,33), where $|\mathcal{K}|\gg1$ [see Eq. (2.25)] and therefore, such a random-phase model is adequate. Ahn and Kim[28] studied this model numerically and found an excellent agreement between the diffusion coefficients found from the random-phase model and from the original separatrix map. (Of course, the random-phase model lacks certain features of the original separatrix mapping, e.g., a rich hierarchical island structure.)

Consider now an ensemble of particles, each having the same total energy E but different initial conditions at $t=0$. In the original problem with Hamiltonian (2.7), we can describe this ensemble by a distribution function (guiding center density) $f(\boldsymbol{\rho},t)$. We will calculate the diffusion coefficient as the coefficient of proportionality between the average particle flux and the average gradient of f in the stationary state. It is convenient to rotate the coordinate system by $\pi/4$. We denote new coordinates by ξ and η. The gradient of f is in the $\hat{\boldsymbol{\eta}}$ direction (Fig. 4).

In fact, the description of the ensemble by function f, which is a function of a vector argument, is reasonable only when we study the exact dynamics. After we have replaced the exact dynamics with that of the separatrix map and now even of the random-phase model, this kind of description became too detailed. Instead, it is sufficient to introduce a set of the distribution functions $f_n^{\pm}(\epsilon)$ of a single argument. Each function in the set represents the deviation of f from its average value at the intersections of the contour $U_0=\epsilon$ with the surfaces of section Σ_n^{ϵ}. The superscripts distinguish between the positive and negative ϵ contours (Fig. 4). Functions f_n^{+} are taken to be zero for $\epsilon<0$ and similarly, $f_n^{-}(\epsilon)=0$ for $\epsilon>0$. We also define ''full'' functions f_n by $f_n(\epsilon)=f_n^{+}(\epsilon)+f_n^{-}(\epsilon)$.

We denote the length of the chessboard cells by d_0 ($d_0=\sqrt{2}\pi d$) and the average gradient $\langle|\nabla f|\rangle$ by $\Delta f/d_0$, then

$$D=\frac{\Phi}{\Delta f}=\frac{\Phi_1-\Phi_0}{\Delta f}, \tag{A1}$$

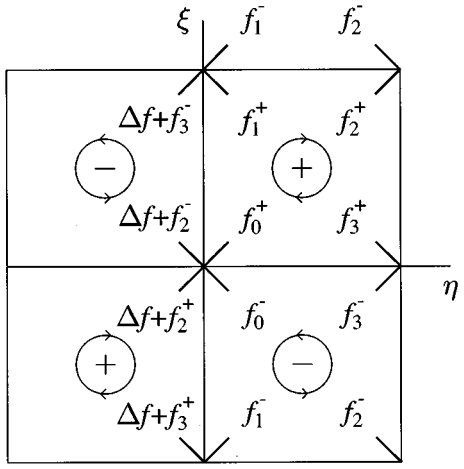

FIG. 4. The chessboard in the coordinate system rotated by $\pi/4$. Pluses and minuses at the centers of the chessboard cells label the maxima and minima of the potential. The direction of the drift velocity is indicated by arrows. Bold segments are the surfaces of section Σ_n^{ϵ}, the same as in Fig. 3. Distribution functions $f_n^{\pm}$ represent the deviation of the guiding center density from the sample averaged value at those parts of Σ_n^{ϵ}'s, which are inside of the two cells on the right. Surfaces Σ_0^{ϵ} and Σ_1^{ϵ} also penetrate the two cells on the left. The corresponding distribution functions are related to $f_2^{\pm}$, $f_3^{\pm}$ as shown.

where Φ is the total flux through the side $\{0<\xi<d_0,\eta=0\}$ and Φ_n is the flux incident upon the Σ_n^{ϵ} surface,

$$\Phi_n=\int_0^{\pi d}dl\,v_d(l)f_n^{+}[\epsilon(l)]=\frac{1}{m\omega_c}\int_0^{W_0}d\epsilon f_n^{+}(\epsilon). \tag{A2}$$

Here l is the coordinate along Σ_n^{ϵ} and $v_d(l)$ is the drift velocity.

To obtain the equation for f_n's note that within the random-phase model, f_{n+1} is quite simply related to f_n. For example,

$$f_2(\epsilon)=\int_0^{2\pi}\frac{d\vartheta}{2\pi}f_1(\epsilon-\Delta\epsilon\,\sin\,\vartheta)=S\bigcirc f_1(\epsilon). \tag{A3}$$

Similarly (see Fig. 4),

$$\Delta f\Theta(-\epsilon)+f_3^{-}(\epsilon)+f_1^{+}(\epsilon)=S\bigcirc[\Delta f\Theta(-\epsilon)+f_2^{-}(\epsilon)+f_0^{+}(\epsilon)], \tag{A4}$$

where $\Theta(x)$ is the step function. Suppose that all f_n's are equal to zero at the center of the cell, then the chessboard symmetry dictates $f_3=-f_1$ and $f_2=-f_0$ and also that functions f_n's are even. These relations can be substituted into Eq. (A4). Then one can eliminate f_0 and obtain an equation solely for f_1,

$$(1+I\bigcirc S\bigcirc I\bigcirc S)f_1(\epsilon)=(I\bigcirc S-I)\Delta f\Theta(-\epsilon), \tag{A5}$$

where $(I\bigcirc f)(\epsilon)\equiv\mathrm{sgn}(\epsilon)f(\epsilon)$. Equation (A5) is an integral equation, in principle solvable by the Winer-Hopf method. However, we have not been able to find its solution analytically. At the same time, a numerical solution is obtained

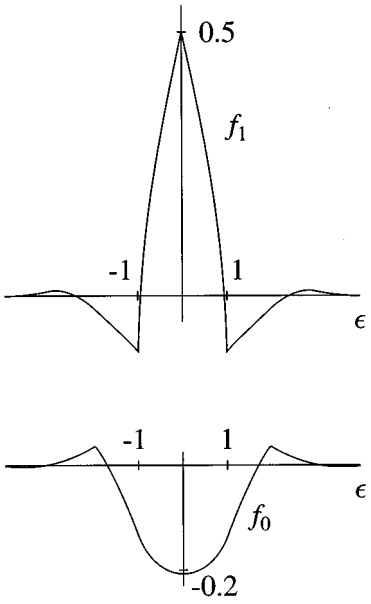

FIG. 5. The distribution functions f_0 and f_1. The density (vertical axis) is in units of Δf and the energy (horizontal axis) in units of $\Delta\epsilon$.

rather easily. The result is shown in Fig. 5. By calculating the area bounded from above by the graph of function f_1, from below by the graph of f_0, and from the left by the vertical line $\epsilon=0$, we have obtained the numerical factor 0.45 in the expression (2.27) for the diffusion coefficient.

Both $f_0(\epsilon)$ and $f_1(\epsilon)$ decay exponentially at $|\epsilon|\gg\Delta\epsilon$. This is in accordance with the statement above that only a narrow boundary layer is important for the transport. Similar to the conventional advection-diffusion problems,[32,33] the width of this layer, $d\Delta\epsilon/W_0$, is of the order of the characteristic displacement of the particle in the direction perpendicular to the flow upon traveling the length of the chessboard's cell.

APPENDIX B: REALISTIC RANDOM POTENTIAL

It has been suggested that a good model for the random potential really existing in GaAs devices is the following one:

$$\tilde{C}(q)=8\pi W^2 d^2 e^{-2qd}, \tag{B1}$$

or equivalently,

$$C(r)=\frac{W^2}{(1+r^2/4d^2)^{3/2}}. \tag{B2}$$

Equations (B1) and (B2) correspond to the potential created in the plane of the two-dimensional electron gas by randomly positioned ionized donors set back by an undoped layer of width d. The amplitude of the potential has the following relation to the parameters of the heterostructure:

$$W^2=\frac{\pi}{8}\frac{n_i(e^2a_B)^2}{d^2}, \tag{B3}$$

where n_i is the density of the donors and a_B is the effective Bohr radius of the electron gas. Equation (B3) applies provided $d\gg a_B$. The random potential can be considered a Gaussian random potential if $n_i d^2\gg 1$.

Using Eq. (B1) for the bare potential, one can also obtain the real-space correlator $C_0(\rho)$ of the averaged potential. Let $R_c\gg d$, then the following relations hold:

$$C_0(\rho)\simeq W_0^2\left(1-\frac{\rho^2}{8d^2}\right), \quad 0\leqslant\rho\lesssim d,$$

$$\simeq W_0^2\frac{4R_c d}{\rho\sqrt{4R_c^2-\rho^2}}, \quad \rho\gtrsim d \quad \text{and} \quad 2R_c-\rho\gtrsim d,$$

$$\simeq W^2\frac{8d^3}{\rho^3}\left(1+\frac{9}{2}\frac{R_c^2}{\rho^2}\right), \quad \rho\gg 2R_c,$$

where

$$W_0=W\sqrt{\frac{2d}{\pi R_c}}.$$

Note that the $1/\rho$ decay of $C_0(\rho)$ for $d\ll\rho\ll R_c$ is a universal feature of $C_0(\rho)$.

APPENDIX C: CALCULATION OF QUASICLASSICAL TRANSITION AMPLITUDES

To derive Eq. (3.3) we start with quantizing the classical Hamiltonian (2.2). The result is

$$\hat{H}=\frac{m\omega_c^2}{2}(\hat{R}_x^2+R_y^2)+U(\hat{\rho}_x+\hat{R}_x,\rho_y+R_y),$$

where hats are used to denote the operators, viz.,

$$\hat{R}_x=il^2\frac{\partial}{\partial R_y}, \quad \hat{\rho}_x=-il^2\frac{\partial}{\partial\rho_y},$$

with $l=\sqrt{\hbar/m\omega_c}$ being the magnetic length. Since the guiding center motion is slow and quasiclassical, we can treat ρ_x as a classical dynamic variable with the equation of motion (2.9) and similarly for ρ_y.

As in Sec. II, we replace the exact trajectory $\boldsymbol{\rho}(t)$ by the ''unperturbed'' one, $\boldsymbol{\rho}_0(t)$. Everything, which was said in Sec. II about the validity of such an approximation, applies here as well.

The Schrödinger equation

$$i\hbar\frac{\partial}{\partial t}\Psi(R_y,t)=\hat{H}\Psi(R_y,t), \tag{C1}$$

where from now on

$$\hat{H}=\frac{m\omega_c^2}{2}(\hat{R}_x^2+R_y^2)+U[\rho_{0x}(t)+\hat{R}_x,\rho_{0y}(t)+R_y]$$

describes the evolution of the cyclotron motion under the influence of time-dependent perturbation $\hat{U}(t)$. The solution of Eq. (C1) will be sought in the form

$$\Psi(R_y,t)=\sum_{M=0}^{\infty} c_M(t)\Phi_M^0(R_y)e^{-i[M+(1/2)]\omega_c t}, \quad \text{(C2)}$$

where function $\Phi_M^0(R_y)$, given by

$$\Phi_M^0(R_y)=\frac{1}{\sqrt{2^M M!\,l}(\pi)^{1/4}}e^{-R_y^2/2l^2}\mathcal{H}_M\left(\frac{R_y}{l}\right),$$

represents the unperturbed wave function of Mth LL ($\mathcal{H}_M$ is the Hermite polynomial). Using this expression, one can find the matrix elements $U_{M,M+k}(t)=\langle M|\hat{U}(t)|M+k\rangle$. If M is large and $|k|\ll M$, then it is sufficient to use the quasiclassical approximation (cf. Ref. 46, Sec. 51)

$$U_{M,M+k}(t)\simeq U_k[\boldsymbol{\rho}_0(t)],$$

where U_k is the Fourier coefficient defined by Eq. (2.8). With the help of this approximation, the equation for the expansion coefficient c_M can be written as follows:

$$i\hbar\frac{dc_M}{dt}=\sum_{k=-\infty}^{\infty} c_{M+k}U_k[\boldsymbol{\rho}_0(t)]e^{-ik\omega_c t}.$$

It has the solution

$$c_M=\int_0^{2\pi}\frac{d\theta}{2\pi}\lambda_0(\theta)e^{-iM\theta}\exp\left(\sum_k S_k(t)e^{-ik\theta}\right),$$

where $\lambda_0(\theta)$ depends on the initial conditions at $t=t_0$ and

$$S_k(t)=-\frac{i}{\hbar}\int_{t_0}^{t}U_k(t')e^{-ik\omega_c t'}dt'.$$

To elucidate the structure of this solution note that formula (C2) can be rewritten in the form

$$\Psi(R_y,t)=\sum_n b_n(t)\Phi_n(R_y,t)e^{-(i/\hbar)E_n t},$$

where the relation of $\Phi_n(R_y,t)$'s to $\Phi_M^0(R_y)$'s is as follows:

$$\Phi_n=\sum_M \Phi_M^0\int_0^{2\pi}\frac{d\theta}{2\pi}e^{i(n-M)\theta}\exp\left[\sum_{k\neq 0}\frac{U_k(t)}{k\hbar\omega_c}e^{-ik(\omega_c t+\theta)}\right].$$

The new expansion coefficients b_n's are given by

$$b_n=\int_0^{2\pi}\frac{d\theta}{2\pi}\lambda(\theta)e^{-in\theta}\exp\left[-\sum_{k\neq 0}\frac{\Delta_k(t_0,t)}{k\hbar\omega_c}e^{-ik\theta}\right], \quad \text{(C3)}$$

where initial conditions now enter through function $\lambda(\theta)$ and $\Delta_k(t_0,t)$ denotes the following integral:

$$\Delta_k(t_0,t)=\int_{t_0}^{t}\dot{U}_k[\boldsymbol{\rho}_0(t')]e^{-ik\omega_c t'}dt'.$$

Functions $\Phi_n(R_y,t)$ represent the ''instantaneous'' LL functions at a given point $\boldsymbol{\rho}_0(t)$ on the drift trajectory. They are the eigenfunctions of $\hat{H}$ with a ''frozen'' value of $\boldsymbol{\rho}_0$. The corresponding eigenvalues E_n, however, turn out to be time independent $E_n=(n+1/2)\hbar\omega_c+U_0$. The transitions between the instantaneous states Φ_n not between the unperturbed states Φ_M^0 have the direct physical meaning. It is the former transition amplitudes we are going to calculate (see a similar discussion in Ref. 46, Sec. 41).

After Eq. (C3) is obtained, we can choose any initial conditions, for instance, $\lambda(\theta)=e^{iN\theta}$ such that $b_n(t_0)=\delta_{n,N}$. In this case $b_{N+k}(t)$ gives the desired $N\to N+k$ inter-LL transition amplitude, i.e., $A_{N,N+k}$ [Eq. (3.3)].

*Permanent address: 194021 St.-Petersburg, Polytekhnicheskaya 26, A. F. Ioffe Institute, Russian Federation.

[1] H. Alfvén, Ark. Mat. Astron. Fys. **27A**, 22 (1940); *Cosmical Electrodynamics* (Oxford University Press, Oxford, 1950).

[2] N. N. Bogolyubov and D. N. Zubarev, Ukr. Mat. Zh. **7**, 5 (1955); M. D. Kruskal, *Proceedings of the Third Conference on Ionized Gases* (Venice, Societá Italiana di Fisica, Milano, 1957).

[3] M. D. Kruskal, J. Math. Phys. (N.Y.) **3**, 806 (1962).

[4] T. G. Northrop, *The Adiabatic Motion of Charged Particles* (Interscience, New York, 1963); B. Lehnert, *Dynamics of Charged Particles* (Elsevier, New York, 1964).

[5] M. Tsukada, J. Phys. Soc. Jpn. **41**, 1466 (1976); S. V. Iordansky, Solid State Commun. **43**, 1 (1982); R. F. Kazarinov and S. Luryi, Phys. Rev. B **25**, 7626 (1982); S. A. Trugman, *ibid.* **27**, 7539 (1983).

[6] *The Quantum Hall Effect*, edited by R. E. Prange and S. M. Girvin (Springer-Verlag, New York, 1990).

[7] Apparently, the first result of this sort was obtained by F. Hertweck and A. Schlüter in Z. Naturforsch. **12A**, 844 (1957). A more detailed analysis, including the calculation of the preexponential factor, can be found in von G. Backus, A. Lenard, and R. Kulsrud, *ibid.* **15A**, 1007 (1960); A. M. Dykhne, Zh. Éksp. Teor. Fiz. **38**, 570 (1960) [Sov. Phys. JETP **11**, 411 (1960)]; **39**, 373 (1960) [**12**, 264 (1960)]; A. A. Slutskin, *ibid.***45**, 978, (1963) [**18**, 676 (1963)].

[8] A similar conclusion was reached previously by D. G. Polyakov (unpublished).

[9] N. Krylov and N. N. Bogolyubov, *Introduction to Nonlinear Mechanics* (Princeton University Press, Princeton, New Jersey, 1974); N. N. Bogolyubov and Y. A. Mitropolsky, *Asymptotic Methods in The Theory of Nonlinear Oscillations* (Gordon and Breach, New York, 1961).

[10] B. Laikhtman, Phys. Rev. Lett. **72**, 1060 (1994).

[11] E. M. Baskin, L. I. Magarill, and M. V. Entin, Zh. Éksp. Teor. Fiz **75**, 723 (1978) [Sov. Phys. JETP **48**, 365 (1978)].

[12] G. M. Zaslavsky, R. Z. Sagdeev, D. A. Usikov, and A. A. Chernikov, *Weak Chaos and Quasi Regular Patterns* (Cambridge University Press, Cambridge, 1991).

[13] See T. Ando, A. B. Fowler, and F. Stern, Rev. Mod. Phys. **54**, 437 (1982) and references therein.

[14] B. Laikhtman and E. L. Altshuler, Ann. Phys. (N.Y.) **232**, 332 (1994).

[15] For review, see P. A. Lee and T. V. Ramakrishnan, Rev. Mod. Phys. **57**, 287 (1985).

[16] For review, see B. Huckestein, Rev. Mod. Phys. **67**, 347 (1995).

[17] D. G. Polyakov and B. I. Shklovskii, Phys. Rev. Lett. **70**, 3796 (1993).

[18] B. I. Shklovskii and A. L. Efros, *Electronic Properties of Doped Semiconductors* (Springer-Verlag, Berlin, 1984).

[19] H. P. Wei, D. C. Tsui, and A. M. M. Pruisken, Phys. Rev. B **33**, 1488 (1985).

[20] D. Weiss, M. L. Roukes, A. Menschig, P. Grambow, K. von Klitzing, and G. Weimann, Phys. Rev. Lett. **66**, 2790 (1991).
[21] R. Fleischmann, T. Geisel, and R. Ketzmerick, Phys. Rev. Lett. **68**, 1367 (1992).
[22] G. M. Zaslavskii and N. N. Filonenko, Zh. Éksp. Teor. Fiz. **54**, 1590 (1968) [Sov. Phys. JETP **27**, 851 (1968)].
[23] B. V. Chirikov, Phys. Rep. **52**, 265 (1979).
[24] D. F. Escande, in *Plasma Theory and Nonlinear and Turbulent Process in Physics*, edited by N. S. Erkohin, A. G. Sitenko, and V. E. Zakharov (World Scientific, Singapore, 1988), p. 398.
[25] J. B. Weiss and E. Knobloch, Phys. Rev. A **40**, 2579 (1989).
[26] A. J. Lichtenberg and B. P. Wood, Phys. Rev. A **39**, 2153 (1989).
[27] V. V. Afanasiev, A. A. Chernikov, R. Z. Sagdeev, and G. M. Zaslavsky, Phys. Lett. A **144**, 229 (1990).
[28] T. Ahn and S. Kim, Phys. Rev. E **49**, 2900 (1994).
[29] V. K. Melnikov, Trans. Moscow Math. Soc. **12**, 1 (1963).
[30] D. V. Treschev, Russ. J. Math. Phys. (to be published); CHAOS **6**, 6 (1996).
[31] J. Greene, J. Math. Phys. (N.Y.) **20**, 1183 (1979).
[32] M. N. Rosenbluth, H. L. Berk, I. Doxas, and W. Horton, Phys. Fluids **30**, 2636 (1987).
[33] B. I. Shraiman, Phys. Rev. A **36**, 261 (1987).
[34] See the review paper, M. B. Isichenko, Rev. Mod. Phys. **64**, 961 (1992), and the references therein.
[35] The diffusion coefficient of a particle traveling in an incompressible flow (Ref. 34) can be obtained from Eq. (2.30) in the following way. The quantity $\Delta\epsilon(a_m)/m\omega_c$ is analogous to the change $\Delta\psi$ of the stream function along the typical trajectory following an optimal cell's perimeter. On the other hand, $\Delta\psi\sim\sqrt{D_s v_d L(a_m)}$ where D_s is the diffusion coefficient in the absence of the flow. For *monoscale* random potential $L(a_m)\sim d(v_d d/\Delta\psi)^{7/3}$. Solving for $\Delta\psi$, we find $D\sim\Delta\psi\sim D_s(v_d d/D_s)^{10/13}$ in agreement with Ref. 34.
[36] M. M. Fogler (unpublished).
[37] A similar result has been obtained previously by D. G. Polyakov, Phys. Rev. B **53**, 15 777 (1996). He finds that the rate of spin-flip processes caused by the spin-orbit interaction for the electrons drifting along the level lines of the random potential is greatly enhanced due to rare places with unusually large drift velocity.
[38] The exact expression for the transport time τ reads
$$\frac{1}{\tau}=\frac{v}{4E^2}\int\frac{\boldsymbol{d}^2\boldsymbol{q}}{(2\pi)^2}|\boldsymbol{q}|\widetilde{C}(\boldsymbol{q}).$$
[39] J. Kucera and P. Streda, J. Phys. C **21**, 4357 (1988); A. Szafer, A. D. Stone, P. L. McEuen, and B. W. Alphenaar, in *Granular Nanoelectronics*, edited by D. K. Ferry, J. R. Barker, and C. Jacoboni (Plenum, New York, 1991); D.-H. Lee, S. Kivelson, and S.-C. Zhang, Phys. Rev. Lett. **68**, 2386 (1992); D. B. Chklovskii and P. A. Lee, Phys. Rev. B **48**, 18 060 (1993); Y. Huo, R. E. Hetzel, and R. N. Bhatt, Phys. Rev. Lett. **70**, 481 (1993).
[40] E. Brézin, S. Hikami, and J. Zinn-Justin, Nucl. Phys. B **165**, 528 (1980); S. Hikami, Phys. Rev. B **29**, 3726 (1982).
[41] A. M. M. Pruisken, in *The Quantum Hall Effect* (Ref. 6), p. 417.
[42] P. Carra, J. T. Chalker, and K. A. Benedict, Ann. Phys. (N.Y.) **194**, 1 (1989).
[43] R. Salomon, Z. Phys. B **73**, 519 (1989).
[44] M. E. Raikh and T. V. Shahbazyan, Phys. Rev. B **47**, 1522 (1993).
[45] M. E. Raikh and T. V. Shahbazyan, Phys. Rev. B **51**, 9682 (1995).
[46] L. D. Landau and E. M. Lifshitz, *Quantum Mechanics: Non-Relativistic Theory*, 3rd ed. (Pergamon Press, New York, 1977).